AD

TECHNICAL REPORT ARCCB-TR-97021

HYDROGEN CRACKING DURING SERVICE OF HIGH STRENGTH STEEL CANNON COMPONENTS

J. H. UNDERWOOD
E. TROIANO
G. N. VIGILANTE
A. A. KAPUSTA
S. TAUSCHER

SEPTEMBER 1997

US ARMY ARMAMENT RESEARCH,
DEVELOPMENT AND ENGINEERING CENTER
CLOSE COMBAT ARMAMENTS CENTER
BENÉT LABORATORIES
WATERVLIET, N.Y. 12189-4050

APPROVED FOR PUBLIC RELEASE; DISTRIBUTION UNLIMITED

DISCLAIMER

The findings in this report are not to be construed as an official Department of the Army position unless so designated by other authorized documents.

The use of trade name(s) and/or manufacturer(s) does not constitute an official indorsement or approval.

DESTRUCTION NOTICE

For classified documents, follow the procedures in DoD 5200.22-M, Industrial Security Manual, Section II-19 or DoD 5200.1-R, Information Security Program Regulation, Chapter IX.

For unclassified, limited documents, destroy by any method that will prevent disclosure of contents or reconstruction of the document.

For unclassified, unlimited documents, destroy when the report is no longer needed. Do not return it to the originator.

REPORT DOCUMENTATION PAGE

Form Approved
OMB No. 0704-0188

1. AGENCY USE ONLY (Leave blank)	2. REPORT DATE	3. REPORT TYPE AND DATES COVERED
	September 1997	Final

4. TITLE AND SUBTITLE
HYDROGEN CRACKING DURING SERVICE OF HIGH STRENGTH STEEL CANNON COMPONENTS

5. FUNDING NUMBERS
AMCMS No. 6226.24.H191.1

6. AUTHOR(S)
J.H. Underwood, E. Troiano, G.N. Vigilante, A.A. Kapusta, and S. Tauscher

7. PERFORMING ORGANIZATION NAME(S) AND ADDRESS(ES)
U.S. Army ARDEC
Benet Laboratories, AMSTA-AR-CCB-O
Watervliet, NY 12189-4050

8. PERFORMING ORGANIZATION REPORT NUMBER
ARCCB-TR-97021

9. SPONSORING / MONITORING AGENCY NAME(S) AND ADDRESS(ES)
U.S. Army ARDEC
Close Combat Armaments Center
Picatinny Arsenal, NJ 07806-5000

10. SPONSORING / MONITORING AGENCY REPORT NUMBER

11. SUPPLEMENTARY NOTES
Presented at the 29th National Symposium on Fatigue and Fracture Mechanics, Stanford, CA, 24-26 June 1997.
Published in *ASTM STP 1332*.

12a. DISTRIBUTION / AVAILABILITY STATEMENT
Approved for public release; distribution unlimited.

12b. DISTRIBUTION CODE

13. ABSTRACT *(Maximum 200 words)*

An investigation of environmental cracking during service of high strength steel cannon components is described. Two cases of cracking occurred in similar prototypes of an advanced cannon over a two-year period. The materials, components configurations, applied and residual stresses, environmental conditions, and the resulting cracking behaviors and SEM fracture surface characteristics are outlined. Laboratory hydrogen cracking tests of the cannon materials, finite element stress analysis, and stress intensity factor calculations were used to model the hydrogen cracking. The first cracking incident involved cracks up to 21-mm long near a pressure seal in an 1160 MPa yield strength ASTM A723 forged steel cannon tube, following five firing cycles. The second incident involved 50-mm long cracks that had grown after thirty firing cycles near the seal between two adjoining cannon components, one made from A723 and one from 1280 MPa yield strength PH 13-8 Mo stainless steel. The cause of cracking, given the presence of hydrogen-laden propellant products and susceptible high strength steels, was the sustained tensile stresses arising from assembly preloads required to maintain pressure seals between cannon components. Recommended preventative measures include reducing the strength level of the existing martensite steels, changing to austenitic nickel-iron base alloys, and redesign to lower the level of sustained tensile stress concentrations in areas subjected to propellant environments.

14. SUBJECT TERMS
Hydrogen Cracking, Pressure Vessels, High Strength Steel, Environmental Cracking Threshold, Crack Growth Rate, Finite Element Analysis

15. NUMBER OF PAGES
20

16. PRICE CODE

17. SECURITY CLASSIFICATION OF REPORT	18. SECURITY CLASSIFICATION OF THIS PAGE	19. SECURITY CLASSIFICATION OF ABSTRACT	20. LIMITATION OF ABSTRACT
UNCLASSIFIED	UNCLASSIFIED	UNCLASSIFIED	UL

TABLE OF CONTENTS

Page

INTRODUCTION 1

COMPONENTS AND CRACKING 1

Configurations and Materials 1

Description of Cracking 2

Firing and Sustained Stresses 4

INTERIM CONCLUSION 6

TESTS AND ANALYSIS 6

Laboratory Hydrogen Cracking Tests 6

Finite Element Analysis 7

Applied *K* at Location #2 7

Discussion 8

CONCLUSIONS 9

Cause 9

Prevention 9

REFERENCES 10

TABLES

1. Measured Material Properties 2

2. Summary of Failure Conditions at Two Locations 4

3. Comparison of Firing and Sustained Stresses at Two Locations 5

LIST OF ILLUSTRATIONS

1. Sketch of Cannon Configuration and Nomenclature 11
2. Sketch of Seal Location #1 and Cracking Observed 12
3. Sketch of Seal Location #2 and Cracking Observed 13
4. Scanning Electron Micrographs of Location #1 Fracture Surfaces 14
5. Hydrogen Cracking for Two Steels; 3000 Hours in Electrolytic Cell 15
6. Scanning Electron Fractographs from Electrolytic Cell Tests 16
7. Finite Element Grid for Analysis of Cracking at Location #2 17
8. Radial Stresses for Location #2 with Average End Load of 156 MPa 17
9. Radial Stresses for Location #2 with Average Seal Load of 3023 MPa 18

INTRODUCTION

During the period 1992 through 1994, a 21-mm long crack was observed in a prototype cannon following five firings, and 50-mm long cracks were observed in a similar cannon following thirty firings . Fatigue cracks are known to develop in cannon components after thousands of firings, but this type of very rapid cracking was unprecedented. Experience with a 1.7-m long environmentally controlled crack in a cannon tube that had experienced no firings (ref 1) suggested environmental cracking as the cause of the cracks of concern here. First, however, an investigation was performed to determine if the cracks observed after up to thirty firings could have been caused by pressure oscillations during firing that had the effect of increasing the effective number of firings. The results (ref 2) showed that many more than the indicated number of stress cycles did occur, but that they were at too low a stress level to have caused the growth of 21- to 50-mm long cracks by mechanical fatigue alone.

The objective here is to describe the observed rapid cracking, some laboratory environmental cracking tests of the cannon materials, and analysis and modeling of the cracking. This information will be used to identify the probable cause of the cracking and to recommend preventative measures for this type of cracking in cannon components. As would be expected, the U.S. Army and its contractors have proprietary interests in the cannon components discussed here. Therefore, limits are applied to some of the discussions here, hopefully in a way that does not interfere with the understanding of the cracking that occurred and its cause and prevention. The approach used in reporting the work is a chronological description of the events and the interim analyses performed and conclusions drawn. Analyses were performed using mean or typical input values, rather than worst case values. If a series of worst case values and assumptions is combined in an analysis, the results will probably be conservative, but such results are often unrealistic and of little use in gaining an understanding of the cause of the event.

COMPONENTS AND CRACKING

Configurations and Materials

The general configuration of the cannon components that sustained rapid cracking is shown in Figure 1. Cannon chamber and tube sections are connected using a cylindrical coupler with segmented threads on its inner surface. As the coupler draws the chamber and tube together, a preload is applied to the pressure seal between the two sections. Two seal locations that have experienced separate occurrences of rapid cracking are described here. Seal location #1, shown in Figure 2, is at a position about midway through the 84-mm wall thickness of chamber and tube. A triangular-shaped copper beryllium seal was used, along with a vented guard ring that allowed pressure on the seal while preventing a direct flow of cannon propellant combustion products onto the seal.

Seal location #2, shown in Figure 3, is at a position near the inner surface of the chamber and tube. A six-sided 17-4 PH stainless steel seal was used in a pocket configured to allow pressure on the seal while, as at location #1, preventing direct flow of propellant products onto the seal contact surfaces. The measured yield and ultimate strengths of the 17-4 PH steel used for the seal at location #2, 984 and 1053 MPa, respectively, were used in the finite element stress analysis discussed later. Strength and fracture properties measured from the 13-8 Mo stainless steel chamber and the ASTM A723 alloy steel tube are shown in Table 1. Fracture toughness was measured using ASTM Method E813 for J_{Ic}, and the hydrogen cracking threshold measurements were performed as described in Reference 3.

Table 1. Measured Material Properties

Material	Yield Strength (MPa)	Tensile Strength (MPa)	Fracture Toughness (MPa $m^{½}$)	Hydrogen Cracking Threshold; 3000 hrs (MPa $m^{½}$)
A723 Grade 1 Alloy Steel	1160	1275	125	10; Electrolytic Cell 16; Acid Solution
PH 13-8 Mo Stainless Steel	1276	1344	145	17; Electrolytic Cell

Additional hydrogen cracking test results are described later.

Description of Cracking

Location #1

Cracking in the prototype cannon with the seal at location #1 was suspected due to a small pressure leak that was observed during the fifth firing cycle. The typical crack size and location sketched in Figure 2 show a 21-mm (surface length) crack that provided a pressure path around the seal and thus accounted for the observed leak. Two other cracks were observed at other angular positions of the seal, a 19-mm surface length crack at a position 185° away from the 21-mm crack, and a 6-mm surface length crack 111° away from the 21-mm crack. The angular positions are significant because the two largest cracks were within a few degrees of alignment with the two 180°-spaced vent holes in the guard ring, and the 6-mm crack was closely aligned with a plugged test hole in the guard ring contact surface of the tube. The presence of the plugged hole could have affected the contact surface and allowed passage of combustion products at this location. Thus, each of the three positions of cracking was closely aligned with angular positions of known (guard ring vent holes) or suspected (plugged hole) sources of propellant combustion products. This is strong evidence that the source of the environment that contributed to the cracking was the combustion products. Regarding initiation of the three cracks, each of the three cracks included the internal corner of the seal pocket adjacent to the seal. This corner is a likely origin of cracking. As shown in Figure 2, the larger two cracks extended farther from the corner toward the outer radius of the tube rather than toward the inner radius; this can be

explained in terms of the residual stresses in the cannon tube, discussed in the next section. The 6-mm crack was nearly centered on the internal seal pocket corner, thus indicating that this seal pocket corner was the origin of the cracks.

The fracture surfaces of the location #1 cracks were characterized using scanning electron microscopy. Figure 4[a] shows an area near the farthest extent of the crack, where the fracture surface was less affected by apparent corrosion products. Even though the surface was partially obscured, the intergranular nature of the fracture can be seen, indicating that environmental cracking had occurred. Figure 4[b] shows the microvoid coalescence fracture that occurred ahead of the area of firing-related cracking when the sample was broken apart.

Location #2

Cracking in the prototype cannon with the seal at location #2 was found to be quite extensive when the cannon was disassembled after thirty firing cycles. Nearly identical crack configurations were observed in both the chamber and tube sections of the cannon, initiating from a location in the seal pocket about 30° from the axial direction in each section; see Figure 3. The cracks extended through to the inner radius surface and extended about 50 mm in the circumferential direction in each section. The similar location, size, and orientation of rapid cracking in components of different material is quite remarkable. The similar cracking suggests that a significant load was applied about equally at locations close to the seal pocket radius of both the chamber and tube, thereby overwhelming the expected differences in cracking resistance of the two materials. Referring again to Figure 3, the seal contact load that is applied to the seal surfaces of the chamber and tube meets this criterion of a significant local load being applied to both cannon sections. The question of whether or not seal contact loads can result in tension stresses in the seal pocket radius will be addressed later, in relation to the finite element results.

Attempts were made to view the location #2 fracture surfaces near the initiation of cracking at the seal pocket radius. However, these fracture surfaces had long since been removed by thermal and chemical action of the combustion products impinging on the crack surfaces during firing. Apparently, after cracks had grown through to the inner radius of the chamber and tube, the direct blast of combustion products quickly obliterated the fracture surfaces.

Summary of Cracking in Locations #1 and #2

Table 2 lists some of the key information related to the cannon firing and the cracking that resulted. Note that the crack orientation at the two locations was different, with radial cracking in the plane normal to the circumferential direction for location #1, and longitudinal cracking in the plane normal to the radial direction for location #2. Note also the difference in radial position of the initiation point of cracking, which will affect the firing and sustained stresses present in the components, considered next.

Table 2. Summary of Failure Conditions at Two Locations

Location	Firing Pressure (MPa)	Number of Firings	Crack Orientation	Radial Position (mm)	Longest Crack Dimension (mm)
#1	405	5	C-R	110	A723: 21
#2	405	30	R-L	86	A723: 50 13-8 Mo: 50

Firing and Sustained Stresses

The firing stress of concern at location #1 is the hoop direction stress in the tube wall, $\sigma_{\theta FIRING}$, since it is normal to the plane of the crack. At location #2, it is the radial direction stress, $\sigma_{R\text{-}FIRING}$. The standard expressions for these stresses are (ref 4)

$$\sigma_{\theta\text{-}FIRING} = p[(r_2/r)^2 + 1]/[(r_2/r_1)^2 - 1] \quad (1)$$

$$\sigma_{R\text{-}FIRING} = -p[(r_2/r)^2 - 1]/[r_2/r_1)^2 - 1] \quad (2)$$

where p is firing pressure, r_1 and r_2 are inner and outer radius, and r is the radial position being considered.

The sustained stresses at the two locations due to the overstrain of the tube are available from Hill (ref 5). As above, the hoop stress relates to location #1 and the radial stress to location #2. The expressions are

$$\sigma_{\theta\text{-}OVERSTRAIN} = \sigma_y[[(r_2/r)^2 + 1]\ [1/(\{r_2/r_1\}^2 - 1)]\ [(r_P^2 - r_2^2)/2r_2^2 - 1n\{r_P/r_1\}] + (r_P^2 + r_2^2)/2r_2^2 + 1n\{r_P/r\}] \quad (3)$$
$$for\ r_1 \le r \le r_P$$

$$\sigma_{R\text{-}OVERSTRAIN} = \sigma_y[[1 - (r_2/r)^2]\ [1/(\{r_2/r_1\}^2 - 1)]\ [(r_P^2 - r_2^2)/2r_2^2 - 1n\{r_P/r_1\}] + (r_P^2 - r_2^2)/2r_2^2 - 1n\{r_P/r\}] \quad for\ r_1 \le r \le r_P \tag{4}$$

where σ_y is the tube yield strength, r_P is the overstrain elastic-plastic radius, and the other terms have been defined. The tube section of the cannon was overstrained in both case #1 and #2 to a nominal 55 percent, that is, $(r_P - r_1)/(r_2 - r_1) = 0.55$. The chamber section was not overstrained in either case.

For the location #2 configuration, another source of nominal sustained stress that could affect cracking at the seal pocket radius is the load on the ends of the tube and chamber sections due to the coupler. In prior work (ref 2) the end load was calculated to be a nominal 156 MPa axial compression that could result in a tensile stress at the seal pocket radius. Later finite element results will show that the end load does result in tensile stress at the radius, but at a relatively low value. The finite element results will also show the important effect of local seal contact loads, mentioned earlier, in causing tensile stress in the seal pocket radius.

A summary of the nominal firing and sustained stresses calculated as above for both locations is shown in Table 3. Since these are nominal stresses, no account has yet been made of stress concentration. Note that the duration of firing stresses is about 0.01 second, which raises the question of whether there is sufficient time for firing stresses to make any contribution to environmental cracking. Also, the firing stresses are compressive at location #2, so could only retard cracking at this location. The nominal sustained stresses due to overstrain (only the tube had overstrain) were tensile only at location #1. Note that the value of tension increases significantly for 45 percent overstrain, which could be within the variation expected for an intended overstrain of 55 percent.

Table 3. Comparison of Firing and Sustained Stresses at Two Locations

Location	Nominal Firing Stress		Nominal Sustained Stress		
	Level (MPa)	Duration (seconds)	Overstrain (%)	(MPa)	Preload (MPa)
Location #1 Hoop Stress	+387	0.01	45 55 65	+107 +35 -20	0
Location #2 Radial Stress	-311	0.01	45 55 65	-58 -67 -73	+156

INTERIM CONCLUSION

At this point in the work, the following interim conclusion was drawn: the cracking in the prototype cannon with the location #1 seal, given an aggressive environment and susceptible material, was caused by the tensile hoop direction overstrain residual stress and the stress concentration at the internal seal pocket corner adjacent to the seal. Based on this conclusion, the location #1 configuration and any further analysis of this location were abandoned. These decisions were based on:

- Work indicating that gun propellant combustion products typically contain hydrogen in significant quantity (ref 6);
- Knowledge that high strength martensitic steels are highly susceptible to hydrogen cracking;
- Presence of sustained tensile stresses due to overstrain at the point of crack initiation, as has been discussed here.

In order to understand the location #2 cracking, further tests and analysis were performed, discussed next.

TESTS AND ANALYSIS

Laboratory Hydrogen Cracking Tests

Laboratory hydrogen cracking tests (ref 3) have been performed in response to the earlier environmental cracking incident (ref 1) and to the cracking under discussion here. Results from the prior work with direct application to the discussions here are shown in Figure 5. Bolt-loaded compact specimens were machined from the tube and chamber sections described here and tested in an electrolytic cell containing a 3.5 percent aqueous NaCl solution containing As_2O_3 poison and using a current density of 40 ma/cm^2. Additional information on the tests is in Reference 3. Crack growth rate from a five-point moving average varies over four orders of magnitude for the two materials. A larger increase in da/dt with increasing applied K was noted for the 13-8 Mo steel, compared with A723. The two materials had about the same da/dt of 10^{-5} mm/s at an applied K of 30 MPa m$^{1/2}$. Since there was a similar amount of observed cracking at location #2 for the chamber and tube cannon sections, it will be interesting to see if this value of 30 MPa m$^{1/2}$ is consistent with the calculation of applied K based on finite element results, described later.

Scanning electron fractography was performed on samples from the hydrogen cracking tests described in Figure 5. Results are shown for the 13-8 Mo and A723 steels in the sustained cracking area affected by environment, Figures 6[a] and 6[b], respectively. The 13-8 Mo fracture surface was quite classic intergranular fracture, typical of hydrogen cracking. The A723 steel also shows clear evidence of intergranular cracking, as well as secondary cracking, both obscured to some degree by corrosion products. More effects of corrosion are expected with the A723 steel

because of its much lower Cr and Ni content. Note also that there is a general similarity between Figure 6[b], from the A723 laboratory tests, and Figure 4[a], from the location #1 failure of the A723 tube section as a result of firing.

Finite Element Analysis

The important unanswered question at this point of the fracture case study was whether or not a significant sustained tensile stress could be accounted for at the location #2 failure location. A finite element analysis was performed to answer this question, using the ALGOR program. The portion of the grid in the area of the seal pocket is shown in Figure 7. The two types of sustained loads discussed previously were considered in the analysis and are shown schematically in Figure 7. The end load is caused by the contact between the chamber and tube sections of the cannon as they are drawn together by the coupler, see again Figure 1. An average end load of 156 MPa was determined from prior work (ref 2), based on typical loads on the coupler threads. The seal load, the other type of loading considered, was determined from the yield and ultimate strengths of the seal material given earlier and the significant values of triaxial stresses that are present in contact stress situations. Based on prior work (ref 7), the contact stresses are 2.97 times larger than the uniaxial yield strength of the material, the lower strength seal material in this case. Using this value of 2.97 and the average of the yield and ultimate strengths of the seal material, 1019 MPa, gives a seal load of 3023 MPa.

Results of the finite element analysis are given in Figures 8 and 9, which show contour plots of the radial direction stresses in the area of the seal pocket. Recall from Figure 3 that the location #2 cracking in both components started within 30° of normal to the radial direction. Figure 8 shows the radial stress distribution resulting from the 156 MPa end load. The maximum radial tensile stress in the seal pocket radius is 12 MPa at an angle of 29° from the radial direction, compared with 30° from the radial direction for the observed cracks in Figure 3. Note that most stresses in the area of the seal pocket are compressive and that the $\sigma = 0$ contour approximates the direction of the observed cracks shown in Figure 3. Figure 9 shows the radial stress distribution resulting from the 3023 MPa seal contact load. The maximum radial tensile stress in the seal pocket radius is 233 MPa at an angle of 14° from the radial direction. As with Figure 8, most stresses in the area of the seal pocket are compressive and the $\sigma = 0$ contour approximates the direction of the observed cracks. It is clear from these results that stresses from both end loads and from seal contact loads can account for the initiation location and the growth directions of the observed cracking, and that the seal contact loads have the more significant quantitative effect on cracking. Next, these results will be used to calculate the approximate value of applied stress intensity factor, for comparison with the measured crack growth rate versus applied K data presented earlier.

Applied K at Location #2

An expression for the applied stress intensity factor at the initiation of cracking at the seal pocket radius can be written based on the well-known short crack K expression and the expression (ref 4) for elastic stress concentration factor, k_t, for a notch, as follows:

$$K_{applied} = 1.12 k_t \sigma_{applied} (\pi a)^{1/2} + 1.12 p (\pi a)^{1/2} \quad (5)$$

$$k_t = 1 + 2(a/r)^{1/2} \quad (6)$$

where 1.12 is the constant for short cracks; $\sigma_{applied}$ is the sum of the end load and seal contact load stresses from the finite element analysis, 245 MPa; p is the firing pressure, 405 MPa; a is the depth of a preexisting notch assumed to be present (due to a machining defect) at the seal pocket radius, 0.1 mm; and r is the radius of the preexisting notch, 0.02 mm. For these values, $k_t = 5.5$ and the two terms of Eq. (5) become:

$$K_{applied} = 26.7 + 8.0 = 34.7 \ MPa \ m^{1/2} \quad (7)$$

The first term in Eqs. (5) and (7) accounts for the maximum sustained tensile stress at the seal pocket radius caused by the end load and seal contact loads and the concentration of this sustained stress by a local defect. The second term in Eqs. (5) and (7) accounts for the pressure in the notch during firing. The sustained stress effects predominate during initiation of cracking, as described in Eq. (7). As the crack grows the sustained stresses diminish, as seen in Figures 8 and 9, and the pressure effect can become predominant. However, as mentioned earlier, the pressure is applied for a very short time, and this may limit its effect in inducing crack growth.

Discussion

The value of applied K determined above, 34.7 MPa $m^{1/2}$, compared with the growth data in Figure 5, can account for the cracking observed at location #2 in both the A723 steel tube and the 13-8 Mo steel chamber. Of course, the value of applied K depends on the assumption of a 0.1-mm deep, 0.02-mm radius defect, but these values are believed to be representative of typical manufacturing methods. Recent work (ref 8) in fatigue initiation with cannon components supports this belief.

It is not known how well the electrolytic cell tests simulate the actual environmental cracking that occurs in the cannon firing environment. It is encouraging that tests conducted using an acid hydrogen cracking environment and the same two steels discussed here (ref 3) give similar crack growth results to those shown in Figure 5.

CONCLUSIONS

Cause

The cause of cracking at location #2 of both the A723 tube and the 13-8 Mo chamber sections of a prototype cannon, given the presence of hydrogen-laden propellant products and susceptible high strength steels, was the sustained tensile stresses arising from assembly preloads required to maintain pressure seals between cannon components. The seal contact load produced a sustained tensile stress in the seal pocket radius near the location of the observed cracking. The end load between the tube and chamber produced a small addition to the sustained tensile stress at the observed cracking location. Firing pressure loads may have contributed to the initiation of cracking and are believed to be the predominate cause of continued growth of the cracks.

Prevention

Recommended preventative measures, given that hydrogen-containing products cannot be avoided, involve either decreasing the cracking susceptibility of the material or reducing the level of sustained tensile stress. Decreased material susceptibility can be attained by reducing the strength level of the existing martensitic steels, or, if possible, by changing to austenitic nickel-iron base alloys. The technical literature, including results in Reference 3, documents the decreases in hydrogen cracking susceptibility that can be obtained.

A reduced level of sustained tensile stress near pressure seals in these cannon components can be accomplished by design changes that reduce stress concentrations near the seal contact area. An increased seal pocket radius and a machining process with smaller inherent defect size would reduce the sustained stresses. A small further reduction in sustained stress can be accomplished by increasing the separation distance between the seal pocket area and areas of end load between cannon components.

REFERENCES

1. Underwood, J.H., Olmstead, V.J., Askew, J.C., Kapusta, A.A., and Young, G.A., "Environmentally Controlled Fracture of an Overstrained A723 Steel Thick-Wall Cylinder," *Fracture Mechanics: Twenty-Third Symposium, ASTM STP 1189*, American Society for Testing and Materials, 1993, pp. 443-460.

2. Troiano, E., Underwood, J.H., Scalise, A., O'Hara, G.P., and Crayon, D., "Fatigue Analysis of a Vessel Experiencing Pressure Oscillations," *Fatigue and Fracture Mechanics: 28th Volume, ASTM STP 1321*, American Society for Testing and Materials, 1997.

3. Vigilante, G.N., Underwood, J.H., Crayon, D., Tauscher, S., Sage, T., and Troiano, E., "Hydrogen-Induced Cracking Tests of High Strength Steels and Nickel-Iron Base Alloys Using the Bolt-Loaded Specimen," *Fatigue and Fracture Mechanics: 28th Volume, ASTM 1321*, American Society for Testing and Materials, 1997.

4. Roark, R.J., and Young, W.C., *Formulas for Stress and Strain*, McGraw-Hill, New York, 1975.

5. Hill, R., *The Mathematical Theory of Plasticity*, Oxford University Press, 1950.

6. Sopok, S., and O'Hara, G.P., "Chemical Factors Associated with Environmentally Assisted Cracking of Generic Gun Systems," *Proceedings of 32nd AIAA/ASME/SAE/ASEE Joint Propulsion Conference,* American Institute of Aeronautics and Astronautics, 1996.

7. Underwood, J.H., O'Hara, G.P., and Zalinka, J.J., "Analysis of Elastic-Plastic Ball Indentation to Measure Strength of High Strength Steels," *Experimental Mechanics*, Vol. 26, No. 4, 1986, pp. 379-386.

8. Underwood, J.H., and Parker, A. P., "Fatigue Life Assessment of Steel Pressure Vessels with Varying Stress Concentration, Residual Stress, and Initial Cracks," *Advances in Fracture Research, Vol. 1,* Pergamon, 1997, pp. 215-226.

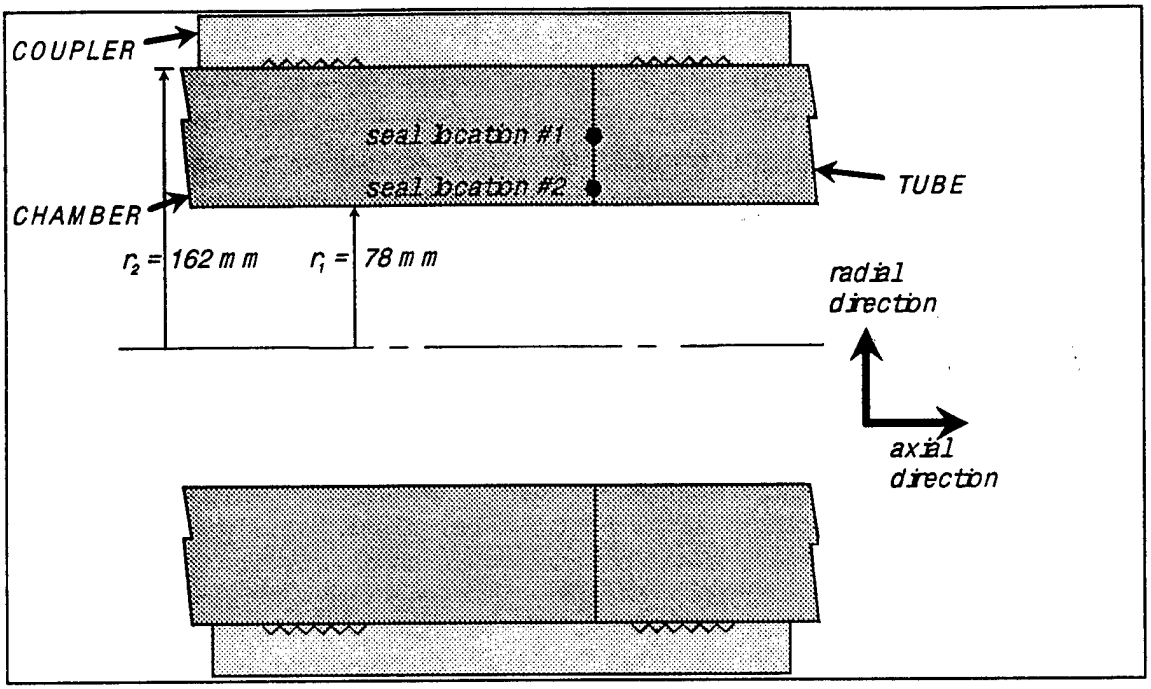

FIG. 1 - Sketch of Cannon Configuration and Nomenclature

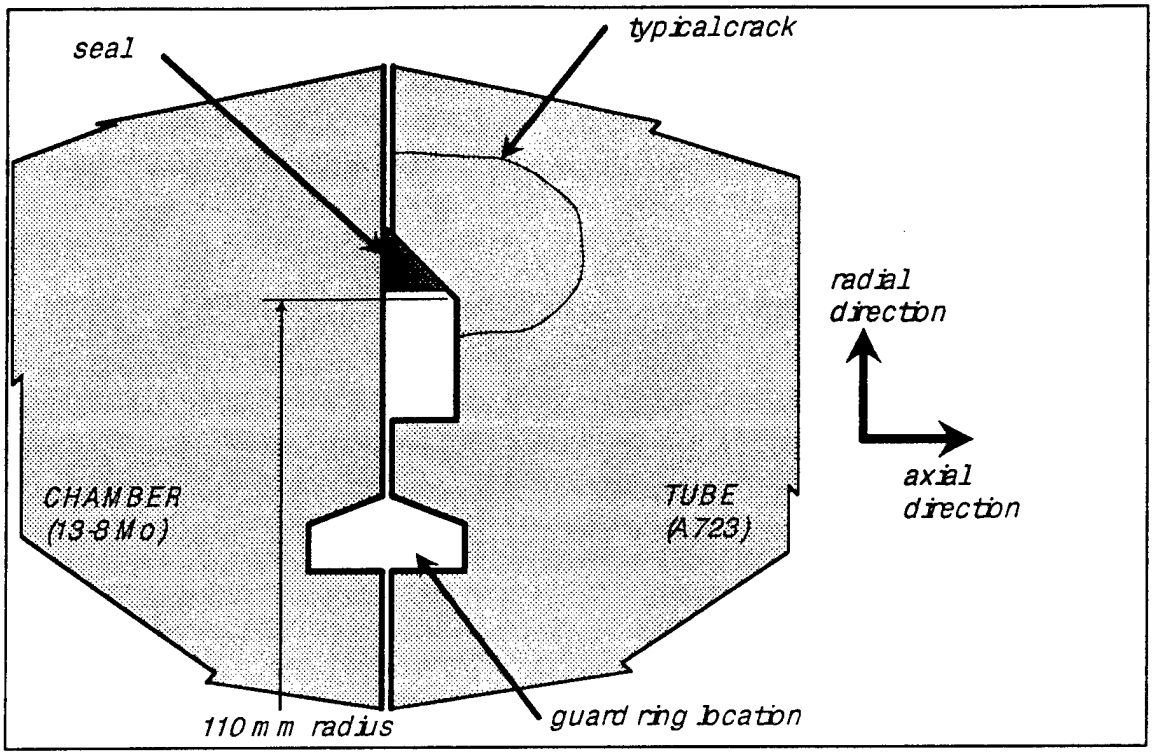

FIG. 2 - Sketch of Seal Location #1 and Cracking Observed

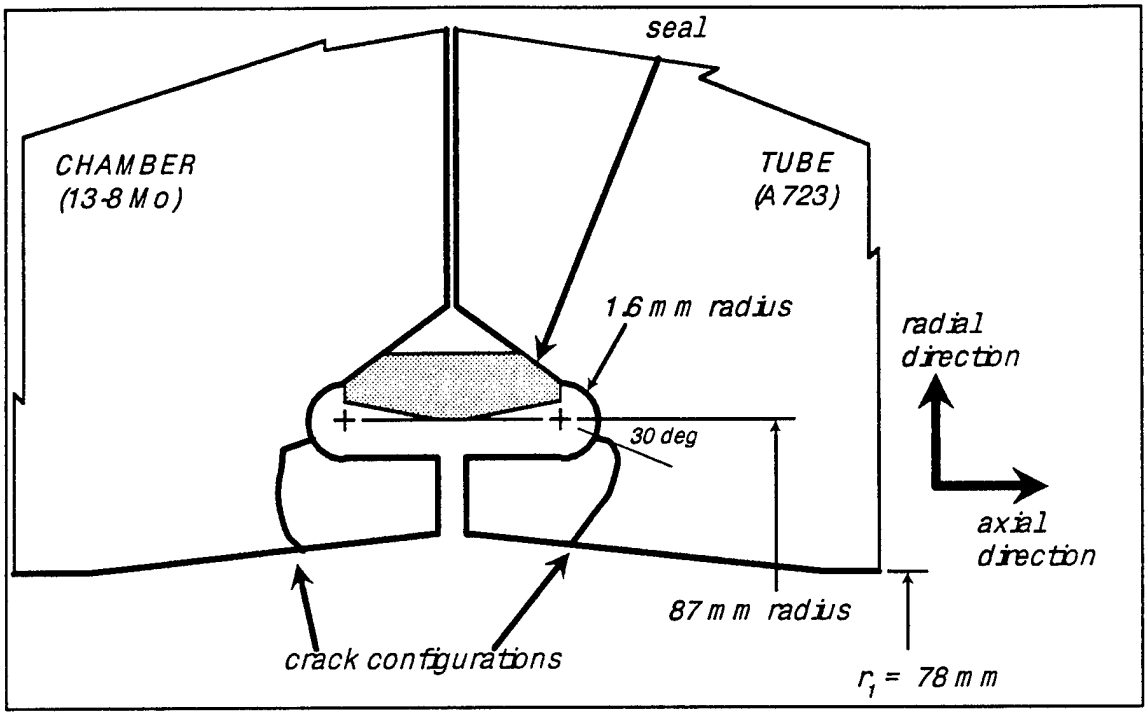

FIG. 3 - Sketch of Seal Location #2 and Cracking Observed

[a]

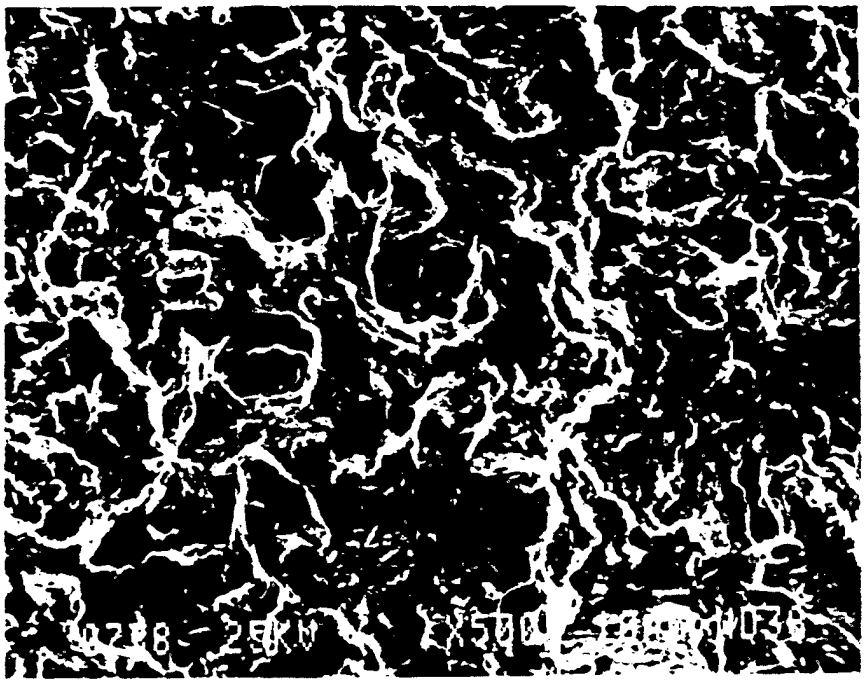

[b]

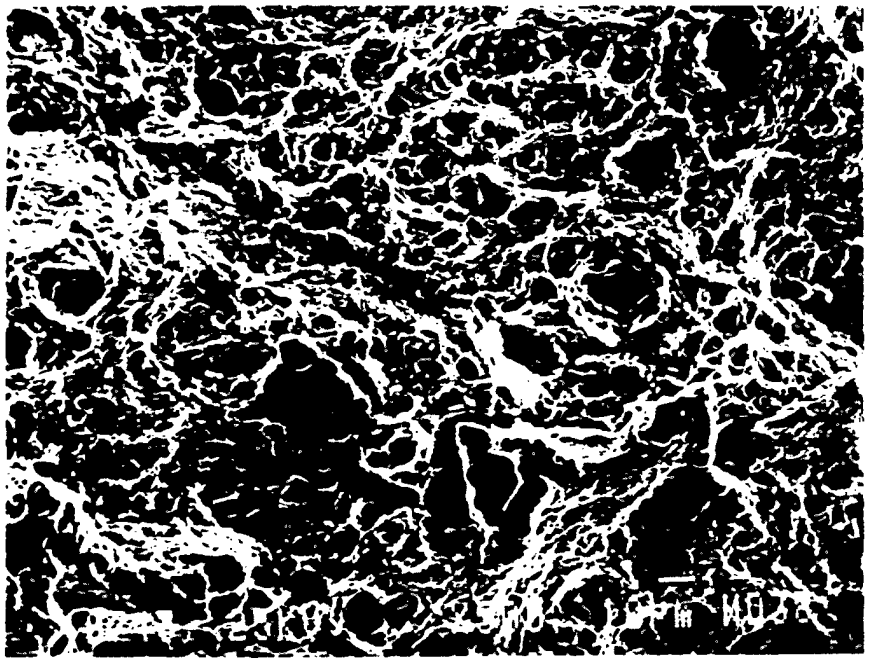

FIG. 4 - Scanning Electron Micrographs of Location #1 Fracture Surfaces; [a] environmental cracking, 500x; [b] ductile fracture for comparison, 500x

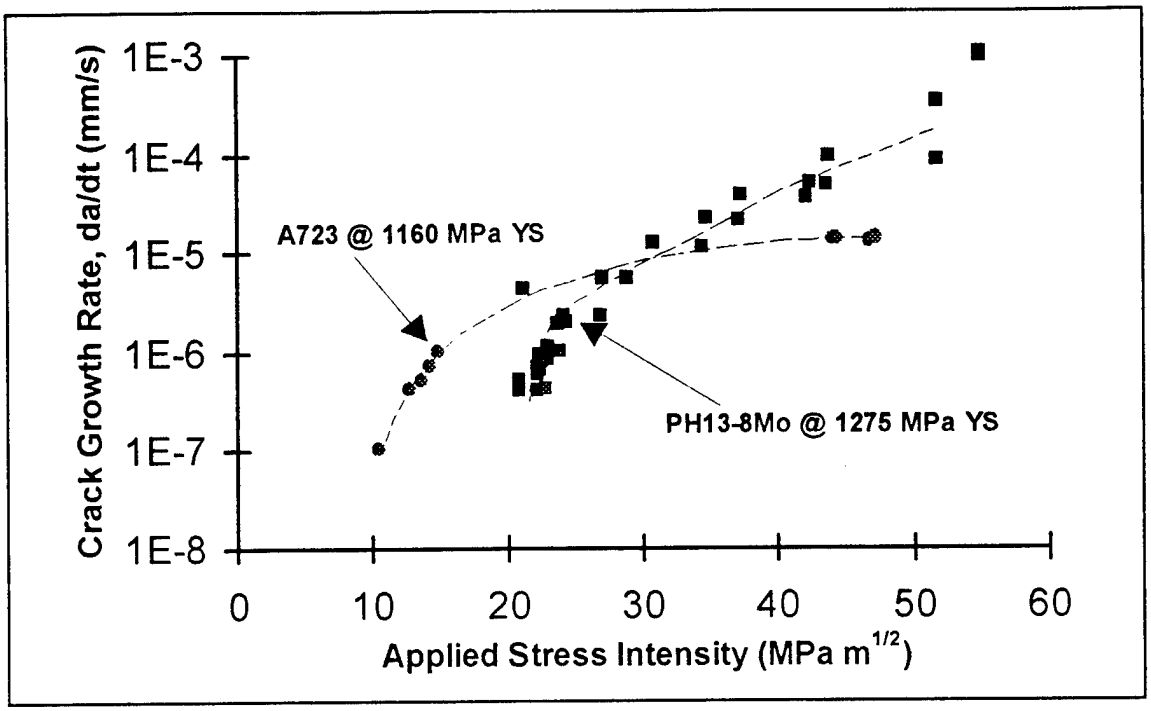

FIG. 5 - Hydrogen Cracking for Two Steels; 3000 hours in Electrolytic Cell

[a]

[b]

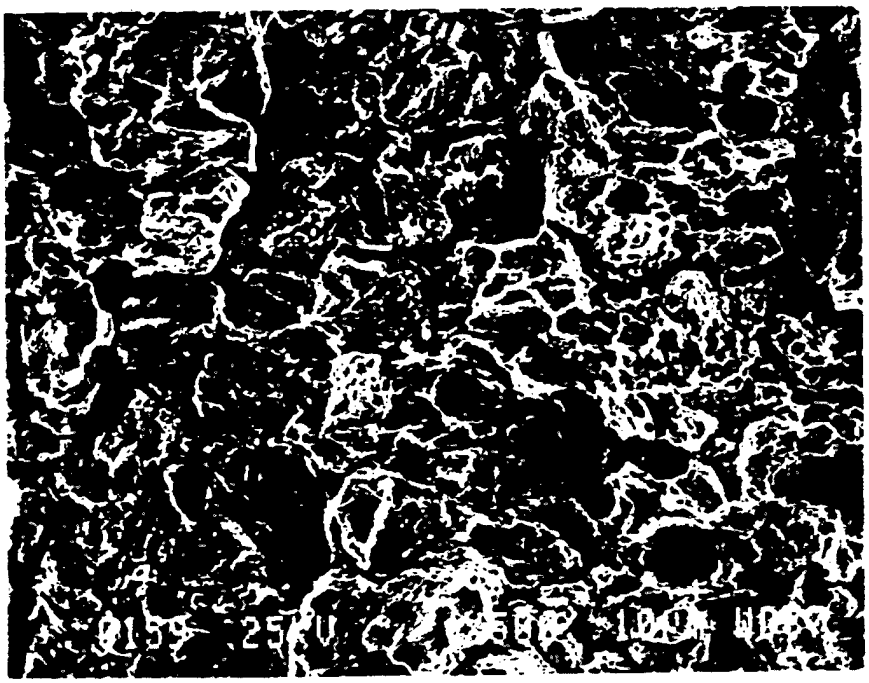

FIG. 6 - Scanning Electron Fractographs from Electrolytic Cell Tests; [a] 13-8 Mo, 500x, 3000 hours exposure; [b] A723, 500x, 3000 hours exposure

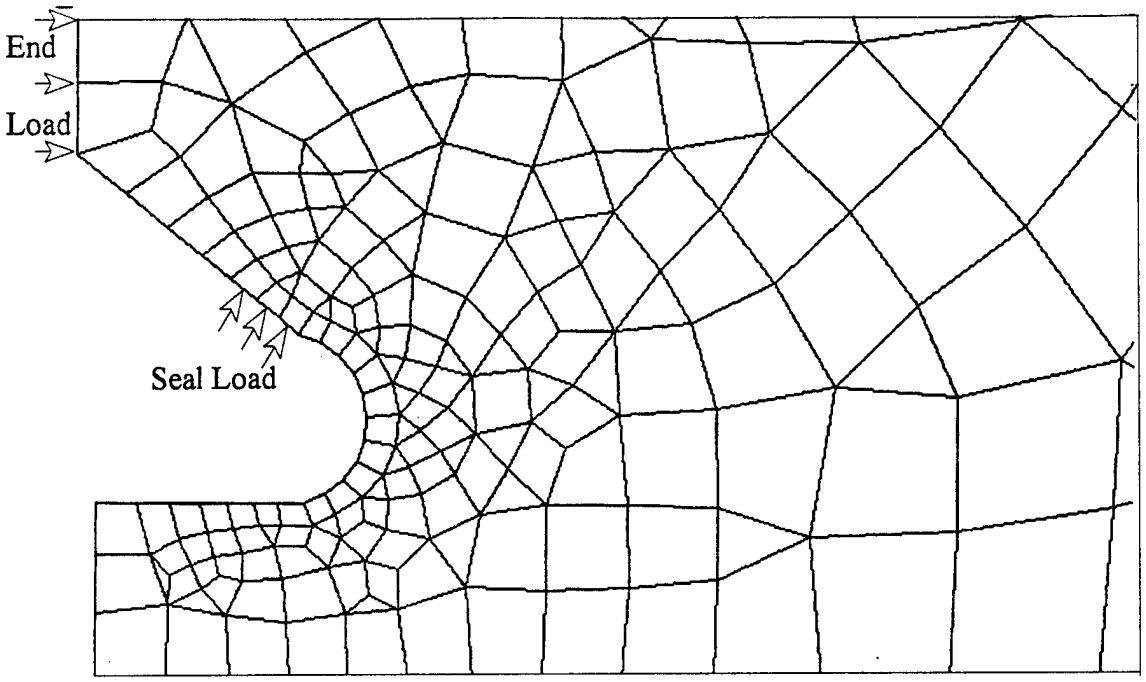

FIG. 7 - Finite Element Grid for Analysis of Cracking at Location #2

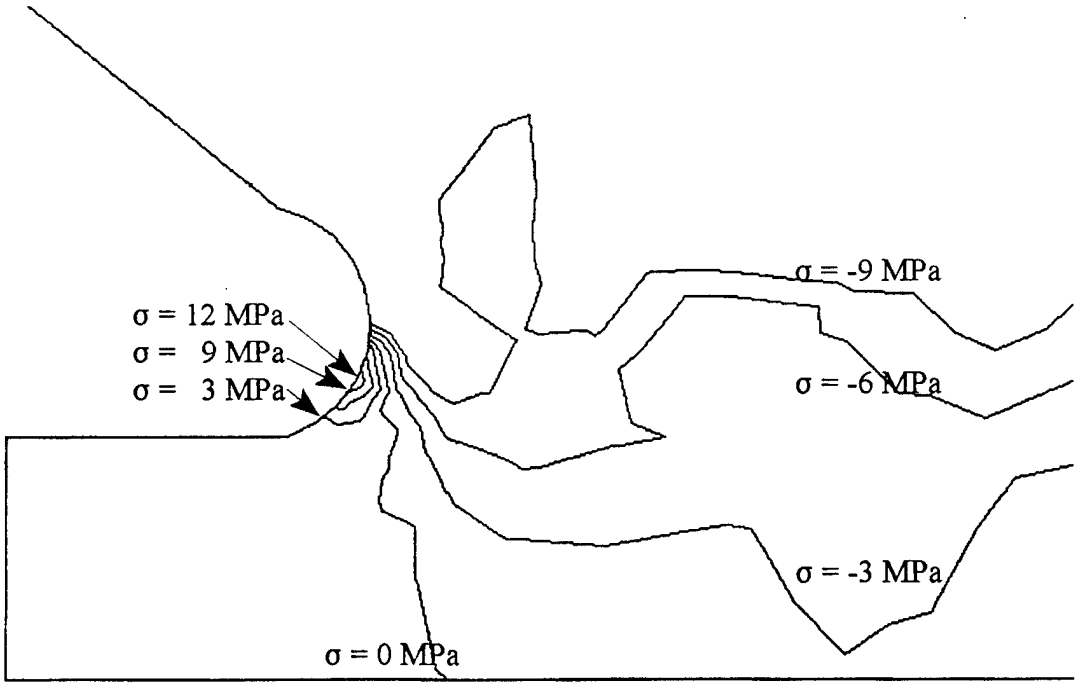

FIG. 8 - Radial Stresses for Location #2 with Average End Load of 156 MPa

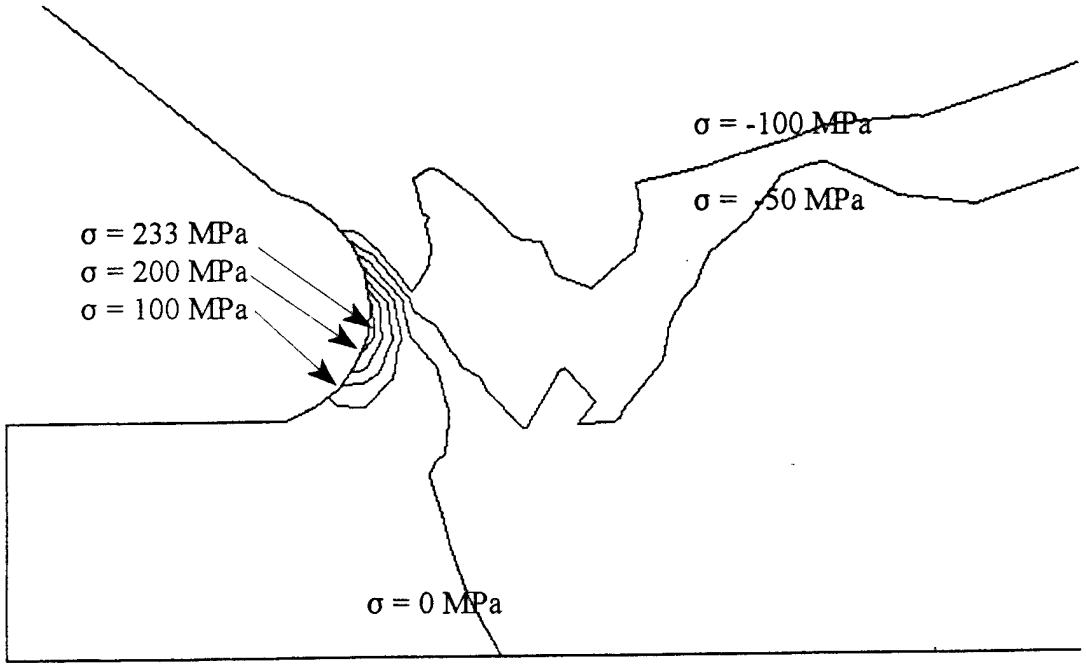

FIG. 9 - Radial Stresses for Location #2 with Average Seal Load of 3023 MPa

TECHNICAL REPORT INTERNAL DISTRIBUTION LIST

	NO. OF COPIES
CHIEF, DEVELOPMENT ENGINEERING DIVISION	
ATTN: AMSTA-AR-CCB-DA	1
-DB	1
-DC	1
-DD	1
-DE	1
CHIEF, ENGINEERING DIVISION	
ATTN: AMSTA-AR-CCB-E	1
-EA	1
-EB	1
-EC	1
CHIEF, TECHNOLOGY DIVISION	
ATTN: AMSTA-AR-CCB-T	2
-TA	1
-TB	1
-TC	1
TECHNICAL LIBRARY	
ATTN: AMSTA-AR-CCB-O	5
TECHNICAL PUBLICATIONS & EDITING SECTION	
ATTN: AMSTA-AR-CCB-O	3
OPERATIONS DIRECTORATE	
ATTN: SIOWV-ODP-P	1
DIRECTOR, PROCUREMENT & CONTRACTING DIRECTORATE	
ATTN: SIOWV-PP	1
DIRECTOR, PRODUCT ASSURANCE & TEST DIRECTORATE	
ATTN: SIOWV-QA	1

NOTE: PLEASE NOTIFY DIRECTOR, BENÉT LABORATORIES, ATTN: AMSTA-AR-CCB-O OF ADDRESS CHANGES.

TECHNICAL REPORT EXTERNAL DISTRIBUTION LIST

	NO. OF COPIES
ASST SEC OF THE ARMY RESEARCH AND DEVELOPMENT ATTN: DEPT FOR SCI AND TECH THE PENTAGON WASHINGTON, D.C. 20310-0103	1
DEFENSE TECHNICAL INFO CENTER ATTN: DTIC-OCP (ACQUISITIONS) 8725 JOHN J. KINGMAN ROAD STE 0944 FT. BELVOIR, VA 22060-6218	2
COMMANDER U.S. ARMY ARDEC ATTN: AMSTA-AR-AEE, BLDG. 3022 AMSTA-AR-AES, BLDG. 321 AMSTA-AR-AET-O, BLDG. 183 AMSTA-AR-FSA, BLDG. 354 AMSTA-AR-FSM-E AMSTA-AR-FSS-D, BLDG. 94 AMSTA-AR-IMC, BLDG. 59 PICATINNY ARSENAL, NJ 07806-5000	1 1 1 1 1 1 2
DIRECTOR U.S. ARMY RESEARCH LABORATORY ATTN: AMSRL-DD-T, BLDG. 305 ABERDEEN PROVING GROUND, MD 21005-5066	1
DIRECTOR U.S. ARMY RESEARCH LABORATORY ATTN: AMSRL-WT-PD (DR. B. BURNS) ABERDEEN PROVING GROUND, MD 21005-5066	1
COMMANDER ROCK ISLAND ARSENAL ATTN: SMCRI-SEM ROCK ISLAND, IL 61299-5001	1
COMMANDER U.S. ARMY TANK-AUTMV R&D COMMAND ATTN: AMSTA-DDL (TECH LIBRARY) WARREN, MI 48397-5000	1
COMMANDER U.S. MILITARY ACADEMY ATTN: DEPARTMENT OF MECHANICS WEST POINT, NY 10966-1792	1
U.S. ARMY MISSILE COMMAND REDSTONE SCIENTIFIC INFO CENTER ATTN: AMSMI-RD-CS-R/DOCUMENTS BLDG. 4484 REDSTONE ARSENAL, AL 35898-5241	2
COMMANDER U.S. ARMY FOREIGN SCI & TECH CENTER ATTN: DRXST-SD 220 7TH STREET, N.E. CHARLOTTESVILLE, VA 22901	1
COMMANDER U.S. ARMY LABCOM, ISA ATTN: SLCIS-IM-TL 2800 POWER MILL ROAD ADELPHI, MD 20783-1145	1

NOTE: PLEASE NOTIFY COMMANDER, ARMAMENT RESEARCH, DEVELOPMENT, AND ENGINEERING CENTER, BENÉT LABORATORIES, CCAC, U.S. ARMY TANK-AUTOMOTIVE AND ARMAMENTS COMMAND, AMSTA-AR-CCB-O, WATERVLIET, NY 12189-4050 OF ADDRESS CHANGES.

TECHNICAL REPORT EXTERNAL DISTRIBUTION LIST (CONT'D)

	NO. OF COPIES
COMMANDER U.S. ARMY RESEARCH OFFICE ATTN: CHIEF, IPO P.O. BOX 12211 RESEARCH TRIANGLE PARK, NC 27709-2211	1
DIRECTOR U.S. NAVAL RESEARCH LABORATORY ATTN: MATERIALS SCI & TECH DIV WASHINGTON, D.C. 20375	1
WRIGHT LABORATORY ARMAMENT DIRECTORATE ATTN: WL/MNM EGLIN AFB, FL 32542-6810	1
WRIGHT LABORATORY ARMAMENT DIRECTORATE ATTN: WL/MNMF EGLIN AFB, FL 32542-6810	1

NOTE: PLEASE NOTIFY COMMANDER, ARMAMENT RESEARCH, DEVELOPMENT, AND ENGINEERING CENTER, BENÉT LABORATORIES, CCAC, U.S. ARMY TANK-AUTOMOTIVE AND ARMAMENTS COMMAND, AMSTA-AR-CCB-O, WATERVLIET, NY 12189-4050 OF ADDRESS CHANGES.